Journal of Applied Geophysics 66 (2008) 31–43

Contents lists available at ScienceDirect

Journal of Applied Geophysics

journal homepage: www.elsevier.com/locate/jappgeo

Inversion of TEM data affected by fast-decaying induced polarization: Numerical simulation experiment with homogeneous half-space

N.O. Kozhevnikov *, E.Yu. Antonov

Institute of Petroleum Geology and Geophysics SB RAS, Prospect Koptyuga, 3, Novosibirsk, 630090, Russia

ARTICLE INFO

Article history:
Received 11 January 2008
Accepted 5 August 2008

Keywords:
TEM method
IP
Inversion
Permafrost

ABSTRACT

A numerical simulation experiment was applied to explore the potential and limitations of the inversion of the TEM response to a uniform half-space with a complex frequency-dependent conductivity described by the Cole–Cole model. The experiment was made by two stages. First we assessed the quality of inversion of 100 m×100 m coincident-loop transient response to a uniform polarizable half-space and then did comparison studies of both separate and joint inversion as applied to the synthetic data for two loop configurations of different sizes. Both of these stages included (1) choice of half-space models and loop configurations; (2) computing synthetic transients and generating pseudo-empirical responses by adding random noise; (3) inversion of pseudo-empirical transients; (4) discussion. During each stage inversion was performed twice: first one of the authors did inversion without any knowledge of the "true" models and then the same author repeated the procedure after he got some prior information from the other author. Inversion of 100 m×100 m coincident-loop transients showed that at low chargeability m and/or exponent c the TEM response can be fitted by the 1D conductive non-polarizable models. Increasing m and/or c resulted in unambiguous IP manifestations even though no prior information was known. More than a half of the recovered models, though some of them differ strongly from the underlying ones, provide a good idea of the "true" ones. The Cole–Cole parameters found by inversion with prior information turned out to approach those of the true models even at low m and c. Joint inversion of data from two loop configurations of different sizes biased effectively the models obtained separately for each configuration toward the true ones. With some prior information, joint inversion provides correct estimates of the Cole–Cole parameters even if the true chargeability is as low as only 0.02. In the case that joint inversion was applied, square error misfit between pseudo-experimental and predicted data was controlled predominately by the fitting error for the very rapidly changing non-monotonous smaller-loop TEM response.

1. Introduction

The effect of induced polarization (IP) in rocks has been largely employed in prospecting surveys, hydrogeology, environmental studies, and also in exploration of frozen ground through the recent decades. Induced polarization phenomenon and IP surveys are widely covered in the literature. From the advent of IP surveys until the 1960–1970s, IP was studied with grounded transmitter and receiver lines, and induction was thought of as noise. That is why IP responses were measured at late times (0.1–1 s after transmitter current turnoff) (Komarov, 1980), when the induction response is almost fully decayed, but IP effects were still measurable. Another reason was that over a long period most of the geophysicists' efforts were focused predominately on slowly decaying mineral grain or electrode IP.

In the early 1970s, the TEM-related publications started to report on non-monotonous, sign reversal included, transients (Spies, 1980; Molchanov et al., 1984; Walker and Kawasaki, 1988). The non-monotonous TEM responses were found to result from induced polarization which decayed much faster than that studied in the conventional IP method (Sidorov and Yakhin, 1979; Lee, 1981; Weidelt, 1983; Molchanov and Sidorov, 1985; Flis et al., 1989).

Understanding that it was fast-decaying IP that was responsible for distortions in monotonic decay of inductive TEM responses prompted the related theoretical research and its application to field TEM measurements. Sidorov and Yakhin (1979), and Kamenetsky et al. (1990) suggested an approximate theory which gave a basic idea of how fast-decaying IP influenced TEM responses.

Nowadays many algorithms and codes for computing IP-affected transients in a horizontally-layered conductive polarizable earth are available based on solutions of pertinent boundary value problems. Most often the response is computed in the frequency domain and then converted into the time domain. Fast-decaying IP is included through the complex frequency-dependent conductivity $\sigma^*(\omega)$,

* Corresponding author.
E-mail address: KozhevnikovNO@ipgg.nsc.ru (N.O. Kozhevnikov).

0926-9851/$ – see front matter © 2008 Elsevier B.V. All rights reserved.
doi:10.1016/j.jappgeo.2008.08.001

commonly with the use of the Cole–Cole model (Lee, 1981; Wait, 1982; Flis et al., 1989; Svetov et al., 1996):

$$\sigma^*(\omega)=\sigma_0\frac{1+(j\omega\tau)^c}{1+(1-m)(j\omega\tau)^c}, \quad (1)$$

where $j=\sqrt{-1}$; ω is the angular frequency, in s^{-1}; σ_0 is the dc conductivity, in S/m; m is the chargeability ($0\le m\le 1$); c is the exponent; τ is the relaxation time, in s.

With today's facilities, computing IP-affected TEM responses of a horizontally-layered earth takes from hundreds of milliseconds to 30 s. The available fast algorithms allows one to see how inductive IP effects change as a function of Cole–Cole parameters, loop configuration, and model geometry. Many relevant publications are rather theoretical discussions (Flis et al., 1989; Kormiltsev et al., 1990; Svetov et al., 1996; El-Kaliouby et. al., 1997) but some report also specific field examples (Descloitres et al., 2000; Kozhevnikov and Antonov, 2006).

While a forward TEM solution for a 1D conductive polarizable earth is no longer problematic, inversion of the IP-effected TEM data still remains to some degree a challenge. Previously much effort was made to separate the inductive and polarization components of the transient process. Studies within the limits of the approximate theory showed that "normal" vortex currents and the polarization currents had different spatial distributions which depended on the loop configuration geometry (Kamenetsky et al., 1990). Therefore, it is possible to enhance or suppress IP effects by changing loop configuration and to some degree to separate the inductive and polarization components by using loops of different geometry at the same site. The possibility of this separation, starting from some delay times or in some interval, underpins a technique proposed recently for "eliminating" the polarization effects from the IP-affected TEM data (Zhandalinov, 2005).

It should be stressed that the separation of inductive and IP responses is possible only as a certain approximation providing polarizability is low and/or polarization and "normal" induction currents decay on a substantially different time scale. The possibilities of such separation are more fully discussed in the paper by Smith et al. (1988). It should be stressed yet that the only general way of inverting IP-affected TEM data is to fit measured TEM response with a synthetic model calculated with regard to frequency dispersion of conductivity and/or dielectric permittivity of the earth. Inversion gives a set of parameters that describes the geological material within the chosen model (e.g., Cole–Cole) in terms of frequency-dependent complex conductivity.

As far as we know, there has not been much literature on inversion of IP-affected TEM data. The few publications are restricted to general considerations (Zadorozhnaya and Lepeshkin, 1998; Svetov et al., 1996) or, at best, display field and model TEM curves in one picture (Descloitres et al., 2000; Krylov and Bobrov, 2002); in the latter case no optimization procedure is applied and synthetic transients are computed for an earth model that the authors just find reasonable. As for the publications concerning inversion of the induction TEM responses affected by fast-decaying induced polarization, they are not available in the relevant literature. The availability of such studies is, however, indispensable to figure out which problems may arise in inversion of TEM data affected by the fast-decaying IP phenomena. We are trying to bridge to some degree the gap by simulating the inversion procedure in a numerical experiment. The reported results provide an idea of potentialities and limitations of TEM data inversion for simple polarizable earth models.

2. Numerical experiment: general approach

So far there has been no object in nature with its electrical properties explored well enough to judge the inversion performance for TEM data affected by fast-decaying IP. Thus we had to generate synthetic data, a procedure not new in itself, but the very numerical experiment has been designed in the way to provide the most faithful simulation of the reality.

Inversion of TEM in terms of polarizable model has to deal with many sought parameters. The number of unknowns in a horizontally-layered earth model can be as great as to hinder structuring and evaluating inversion results because of the equivalence problem. That is why we restricted the modeling to a uniform polarizable half-space. Although being simple, this model is in many respects fundamental in geophysics. It was used earlier to investigate how variations in loop size and in parameters of the ground exhibiting the Debye-type of polarization show up in the TEM response (Flis et al., 1989; Kozhevnikov and Artemenko, 2004; Kozhevnikov and Antonov, 2006).

The frequency dependence of conductivity in our experiment was accounted for using the Cole–Cole model, the parameters of which were selected with reference to real ion-conductive frozen rocks, for several reasons. The primary reason was that non-monotonous transient responses as evidence of fast-decaying IP were often reported from northern areas (Molchanov and Sidorov, 1985; Walker and Kawasaki, 1988; Smith and Klein, 1996; Vanchugov and Kozhevnikov, 1998; Zadorozhnaya and Lepeshkin, 1998; Krylov and Bobrov, 2002; Zhandalinov, 2005). The mechanisms responsible for fast-decaying polarization of frozen ground at early times remained open to discussion (Molchanov and Sidorov, 1985; Sidorov, 1987; Frolov, 1988; Artemenko and Kozhevnikov, 1999; Krylov and Bobrov, 2002; Bitteli et al., 2004) but the very existence of this effect was confirmed by many field and laboratory experiments, including measurements with galvanic arrays (Kozhevnikov et al., 1995; Shesternev et al., 2003; Karasev et al., 2004). Another reason was that we possessed a large collection of field TEM data from West Yakutiya where fast-decaying IP effects still present a considerable challenge to the geophysicists (Vanchugov and Kozhevnikov, 1998; Zhandalinov, 2005; Kozhevnikov and Antonov, 2006).

The experiment consisted of *two stages*. At the first stage we were to get a rough but exhaustive idea of errors in a single inversion of coincident-loop transient response to a polarizable half-space. At the next stage, we applied computer simulation to judge the performance of joint inversion of responses from two different loop configurations. Each stage included (1) computing synthetic transient responses and generating pseudo-empirical transients by adding random noise; (2) inversion of pseudo-empirical transients; (3) discussion.

One of us (referred further as "Author#1") chose the "true" models and computed synthetic transients and the other (referred further as "Author#2") inverted them in terms of a polarizable earth model. Although one often starts geophysical surveying having very little if any prior information, one still has to find a model reasonably fitting the measured data. It is important in such a situation to appreciate the extent of ambiguity of the inversion results. As will soon become evident, in the case that true model is represented by a homogeneous moderately polarizable half-space, the inversion without prior knowledge may result in horizontally-layered models which perfectly fit the measured data. To elucidate what degree of ambiguity one can expect in such a situation, at each of the above two stages inversion was first run when Author#2 had no prior information on the underlying "true" models. Thereupon he was told a portion of information on the underlying models and the inversion was run once again.

The synthetic IP-affected TEM responses were computed using the Unv_QQ code designed by E. Antonov. At first, we tested the Unv_QQ code numerical results by correlating them with those obtained with the SIRO code kindly offered by Professor P. Weidelt, its author. In both codes, written in FORTRAN, the time-domain solution was presented as the Fourier integral of the frequency-domain solution. The frequency-domain solution and the inverse Fourier transform were performed by means of linear filtering.

The SIRO code was designed to compute coincident-loop transients for a coincident-loop laid on the surface of a 1D earth with frequency-

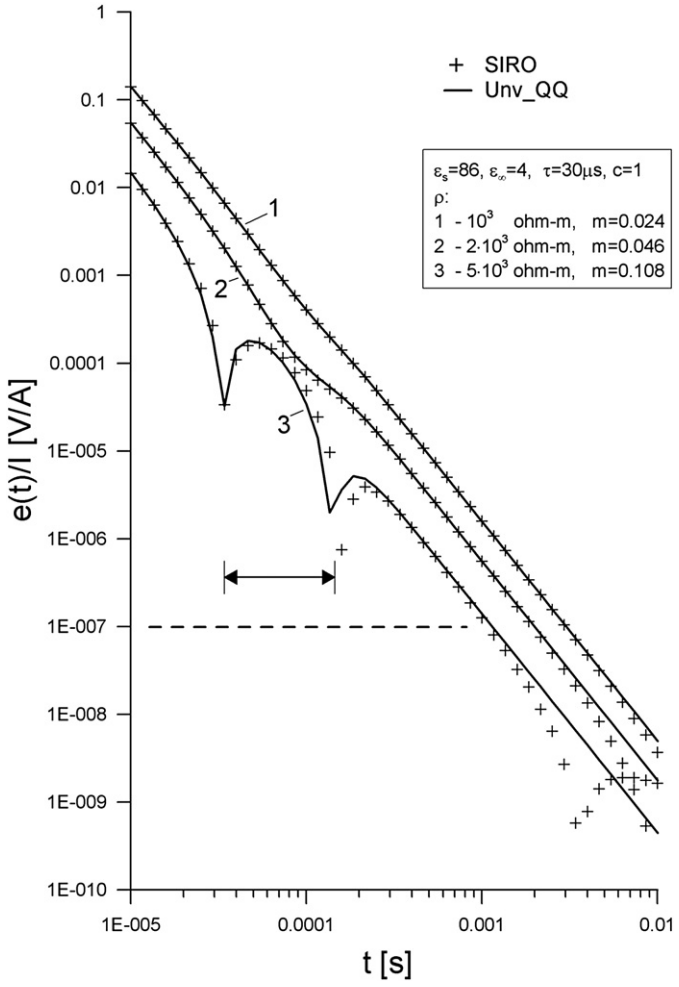

Fig. 1. Comparison of 100 m×100 m coincident-loop transient responses to a homogeneous conductive polarizable half-space computed using the SIRO and Unv_QQ codes. Arrows indicate the time interval of negative response for a $5\cdot10^3$ Ω m half-space. The dashed line marks the noise level typical of a field acquisition system.

independent (ohmic) conductivity σ_0 and frequency-dependent complex permittivity $\varepsilon^*(\omega)$ described by the Debye relaxation model:

$$\varepsilon^*(\omega)=\varepsilon_0\left(\varepsilon_\infty+\frac{\varepsilon_s-\varepsilon_\infty}{1+j\omega\tau}\right), \tag{2}$$

where ε_0 is the free-space dielectric constant ($8.84\cdot10^{-12}$ F/m); ε_s, ε_∞ are the relative static and dynamic permittivities, respectively; and τ is the time constant of dielectric relaxation, in s.

In the frequency and time ranges which the induction prospecting methods commonly operate over, using Eq. (2) to describe polarization of rocks via the conductivity σ_0 and complex permittivity ε^* is the same as using Cole–Cole Eq. (1) with $c=1$, and the chargeability

$$m=\left[1+\frac{\sigma_0\tau}{\varepsilon_0\Delta\varepsilon}\right]^{-1},$$

where $\Delta\varepsilon=\varepsilon_s-\varepsilon_\infty$ is the difference between static and dynamic permittivities (Kozhevnikov and Antonov, 2006).

Some representative computing results for the SIRO and Unv_QQ codes are compared in Fig. 1. The graphs coincide over most of the time range but diverge at late delay times. The discrepancy grows with time and becomes notable earlier at higher resistivities. It shows up especially at times where the normalized transient emf becomes less than 0.1 μV/A which is generally below the overall noise level.

External EM and internal (instrumental) noises are always present in field transients. We accounted for external EM noise by generating a sequence of normally distributed random numbers. The arithmetic mean μ_n of the sequence was always unity ($\mu_n=1$) and the mean-square deviation σ_n was assumed to have a value typical of the measurement error for certain loop configuration. At each time delay, the synthetic transient emf was multiplied by a random number from the generated sequence, thus resulting in pseudo-empirical transient voltages 'measured' with relative mean-square error of σ_n.

Unlike the external EM noise, the instrumental noise, being not dependent on the electromagnetic environment, transmitter moment and the loop configuration, remains the same for a specific TEM-measuring system. We simulated the instrumental noise by adding to the 'measured' voltage the Gaussian noise with a zero mean and absolute mean-square deviation of 0.1 μV. Additive noise was of no importance at early times when the signal was high but strongly distorted the late-time 'tails' of TEM responses.

The inverse problem was solved by fitting a vector **P** from the space **M** of model parameters to provide the minimum of the objective function $\varphi(\mathbf{P})$:

$$\varphi(\mathbf{P})=\left\{\frac{1}{N-1}\sum_{i=1}^{N}\left[\frac{e^{\text{meas}}(t_i)-F_P(t_i)}{\delta(t_i)e^{\text{meas}}(t_i)}\right]^2\right\}^{1/2}, \tag{3}$$

where t_i is the ith time delay; N is the total number of time delays; $e^{\text{meas}}(t_i)$ is the transient emf measured at the ith time delay; F_p is the forward operator; $\delta(t_i)$ is the relative measurement error at the delay t_i. The objective function is the root-mean-squared of weighted differences between the computed and pseudo-empirical transient responses. The set of model parameters is the vector $\mathbf{P}=(\sigma_j,h_j,m_j,\tau_j,c_j)|_{j=1,\ldots,M}$, where M is the total number of layers, σ_j is the conductivity, h_j is the layer thickness, m_j is the chargeability, τ_j is the IP relaxation time constant, and c_j is the exponent for the jth layer. A modified algorithm by Nelder and Mead (1965), that does not require the computation of the derivatives of the forward problem operator, was used to find a minimum of the objective function (3).

Although it was the objective function that was minimized during the inversion, in representing the inversion results we, following a common practice (Spies and Frischknecht, 1991), used the relative root mean-square deviation between 'measured' and modeled data. Unlike the objective function, the root mean-square deviation not only shows how appropriate the model is but also indicates directly the measurement errors provided the model giving an optimal value of the objective function has been found.

3. Numerical experiment: first stage

As we mentioned, at the first stage we applied numerical modeling to study potentialities and limitations of the single inversion of coincident-loop TEM response to a polarizable earth. A good choice of reference models being a main prerequisite of success, forty models of a uniform polarizable half-space with different Cole–Cole parameters (listed in Table 1)were used to get an idea on how they do effect the TEM response.

The dc resistivity ρ of each model was assumed to be 10^3 Ω m. On the one hand resistivities of this order of magnitude are typical of many frozen unconsolidated rocks (Frolov, 1998), and on the other

Table 1
The Cole–Cole parameters of the half-space models used to calculate 100 m×100 m coincident-loop TEM responses

ρ, Ω m	1000
m	0.01, 0.02, 0.05, 0.1, 0.2, 0.5, 0.7, 0.9
τ, s	$5\cdot10^{-5}$
c	0.2, 0.5, 0.7, 0.9, 1

hand such resistivities are sufficiently high to provide an appreciable contribution of chargeability, even of a low one, to the TEM response.

The IP relaxation time constant was held fixed at $\tau = 50$ μs which is typical of unconsolidated frozen rocks at not-too-low negative temperatures (Frolov, 1998; Artemenko and Kozhevnikov, 1999; Bittelli et al., 2004; Kozhevnikov and Antonov, 2006).

Deciding on the likely chargeabilities was problematic. According to early-time IP surveys (Kozhevnikov et al., 1995) m is of the order of =0.1–0.4 in frozen sand. In-situ measurements on frozen sand have demonstrated a correlation between high chargeabilities measured galvanically at times about 100 μs and inductively-induced IP effects in the TEM data (Kozhevnikov et al., 1995). Unfortunately, very few reports provide direct comparison of galvanic and TEM measurements at the same site or in the same geological body. The largely published conventional IP data are useless in our case because reported time range is shifted too far to late times. Being aware of this uncertainty, we used m in a range of 0.01 to 0.9 in order to get an idea on how chargeability manifests itself in the TEM data and in the inversion results. For the same reason, the exponent c was allowed to vary from 0.2 to 1.

At this stage, we computed the TEM responses of a uniform polarizable half-space for a 100 m×100 m coincident-loop configuration. Loops about this size have been widely used in TEM surveys, specifically in kimberlite prospecting in Yakutiya (Vanchugov and Kozhevnikov, 1998; Zhandalinov, 2005). The time range of calculations correspond to the modern TEM instrumental facilities. In actual practice, the earliest measurement time with 100 m×100 m coincident-loop configuration is usually to above 10 of microseconds and to our knowledge is never below 10 μs (Vanchugov and Kozhevnikov, 1998). The accuracy of TEM measurements at late times depends both on the transmitter loop moment and EM noise. The latest time is usually from about ten to a few hundred milliseconds for relatively low resistive rocks ($\rho = 10$–10^2 Ω m) and from a few hundred microseconds to a few milliseconds for more resistive rocks ($\rho = 10^3$–10^4 Ω m).

The relative standard error due to the external EM noise, from experience with 100 m×100 m coincident-loop field data, was assumed to be 5%. Thus the random-number sequence that was mentioned above used to account for the external EM noise had $\mu_n = 1$, and $\sigma_n = 0.05$.

Author#1 computed the synthetic transients and passed them to Author#2 who first ran the inversion without having any priori knowledge of the models and then repeated the procedure after being told that every model was represented by a uniform half-space with resistivity of 10^3 Ω m.

For the models, loop configurations, and noise used in our experiment the signal/noise ratio at times above 1–2 ms became very low and therefore the inversion was applied to data from the time interval 10 μs to about 2 ms. The average squared fitting errors obtained without and with prior information are given in Table 2.

Table 2
Relative mean-square deviation (in %) between pseudo-experimental and predicted 100 m×100 m coincident-loop transient voltage responses obtained when inversion was done without (gray columns) and with prior information.

m	$c = 0.2$		$c = 0.5$		$c = 0.7$		$c = 0.9$		$c = 1$	
0.01	5.4	5.4	5.4	5.4	5.5	5.5	5.9	5.4	6.4	5.5
0.02	5.4	5.4	5.4	5.4	5.7	5.4	5.4	5.4	6.0	5.5
0.05	5.3	5.5	5.4	5.5	5.3	5.4	65	5.4	7.1	5.4
0.1	5.5	5.5	5.6	5.8	5.5	5.6	13	5.4	4.6	4.6
0.2	5.7	5.8	9.7	32	5.6	7.9	17	5.3	16	5.5
0.5	14	7.2	5.9	6.0	8.9	6.8	23	6.0	8.2	5.5
0.7	8.3	5.9	7.9	6.0	6.9	6.2	23	8.0	19	6.1
0.9	9.1	5.7	6.7	5.6	6.9	5.9	39	12	62	12

4. Results

Inversion *without prior information* began with attempting to match pseudo-experimental TEM data with those calculated for models represented by a non-polarizable horizontally-layered conductive earth. Only if those models failed in fitting the pseudo-empirical TEM response, Author#2 tried to fit pseudo-experimental TEM data introducing into the model a polarizable layer. For the sake of convenience, we analyzed the results separately for five groups of "correct", or "true", models distinguished according to the exponent c.

In the case that the effect of fast-decaying IP was not strong enough to be clearly seen in the TEM data, the transient voltage response was converted into apparent resistivities (Fig. 2) using a well-known late-time formula (Kaufman and Keller, 1983)

$$\rho_a(t) = \left[\frac{IS_tS_r}{e(t)20\pi\sqrt{\pi}}\right]^{2/3}\left(\frac{\mu_0}{t}\right)^{5/3}.$$

In this formula, ρ_a is apparent resistivity (Ω m); I is the transmitter loop current (A); S_t is the transmitter loop area (m^2); S_r is the receiver loop area (m^2); t is time (s); $e(t)$ is the voltage induced in a receiver loop (V); $\mu_0 = 4\pi\times10^{-7}$ H/m.

Group 1 (c=0.2): two- or three-layer non-polarizable earth models allowed fitting the pseudo-experimental data at m from 0.01 to 0.2. For models with m=0.01–0.1, apparent resistivity varied in a range of 15–20% and thus there was no need to assume the presence of fast-decaying IP. The transient response for m=0.2 was inverted twice, with the assumptions of a non-polarizable and a polarizable earth, respectively. As Fig. 2a suggests, in this case polarizable and non-polarizable models appeared to be equivalent. Since at m>0.2 TEM responses exhibited a sign reversal which is a characteristic feature of a polarizable earth (Weidelt, 1983) the pseudo-experimental data for m>0.2 were inverted on the basis of 1D polarizable earth model.

Group 2 (c=0.5): models of non-polarizable conductive earth could fit the pseudo-empirical data at m=0.01 – 0.1. At m=0.2, the inversion gave an unrealistic model with very high layer resistivity contrasts (Fig. 2b). The presence of polarizability was hypothesized as at late times the pseudo-empirical apparent resistivity curve became progressively steeper. A layered earth model with a polarizable upper layer gave a much better fit to the pseudo-empirical data (Fig. 2b).

Group 3 (c=0.7): models of non-polarizable two- or three-layer conductive earth could fit the pseudo-empirical TEM responses at m=0.01–0.1. At m=0.1, an equally good fit was obtained with models of both a non-polarizable three-layer earth and a polarizable uniform half-space (Fig. 2c). It was impossible to fit the data with non-polarizable models at m≥0.2: transient voltage double sign reversal indicated conclusively that fast-decaying IP phenomenon had to be incorporated into the model as well as the exponent c being above 0.5 (Kormiltsev et al., 1990).

Group 4 (c=0.9): models of non-polarizable two- or three-layer conductive earth could fit the "measured" data at m=0.01 to 0.05. At m=0.1, the slopes of the "measured" apparent resistivity curve were too steep to be accounted for by a non-polarizable model (Fig. 2d). At m>0.1, double sign reversal in the transient voltage response was evidence that the earth was polarizable and exponent c was above 0.5 (Kormiltsev et al., 1990).

Group 5 (c=1): models of non-polarizable conductive earth could fit the data only at m=0.01 and m=0.02. At m=0.05, non-polarizable earth fitted no transient; fitting results for a polarizable model are illustrated in Fig. 2e. Double sign reversal at m>0.05 indicated obvious necessity to include fast-decaying IP.

The inversion that was repeated *with allowance made for prior information* resulted in a generally better fit of the models to the pseudo-experimental TEM responses (compare Fig. 2f and e). Unlike the previous results, the repeated procedure gave models the

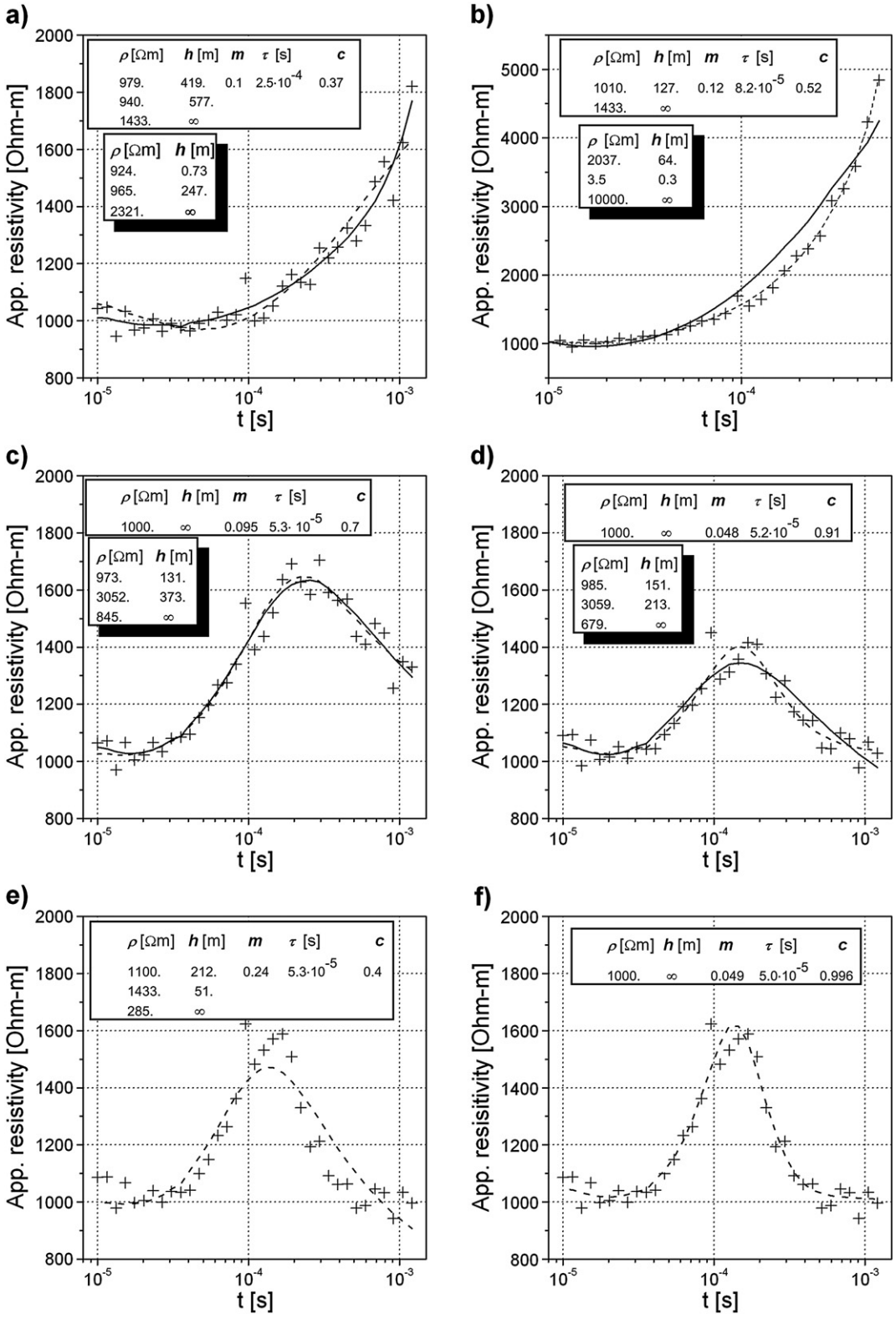

Fig. 2. Results of inversion done without (a–e) and with (f) prior information. Crosses mark pseudo-experimental apparent resistivity curves and lines present those derived through inversion done in the framework of non-polarizable (solid line) and polarizable (dashed line) earth models. Inversion results are in non-shaded boxes for polarizable and in shaded boxes for non-polarizable models. All "correct", or "true", models were represented by homogeneous half-space with $\rho = 10^3$ Ω m, $\tau = 5 \cdot 10^{-5}$ s. Other parameters of "true" models were $c = 0.2$, $m = 0.2$ (a); $c = 0.5$, $m = 0.2$ (b); $c = 0.7$, $m = 0.1$ (c); $c = 0.9$, $m = 0.1$ (d); $c = 0.9$, $m = 0.05$ (e, f).

parameters of which made up a data array with certain systematic patterns. Although the mere fact that those patterns did exist was evident, a way of readily illustrating and generalizing these patterns was not apparent immediately. Eventually, we represented the inversion results as graphs, on the abscissa of which one of the true Cole–Cole parameters (e.g., chargeability m) considered as an independent variable was plotted whereas one of the parameters found through the inversion was displayed on the vertical axis. This

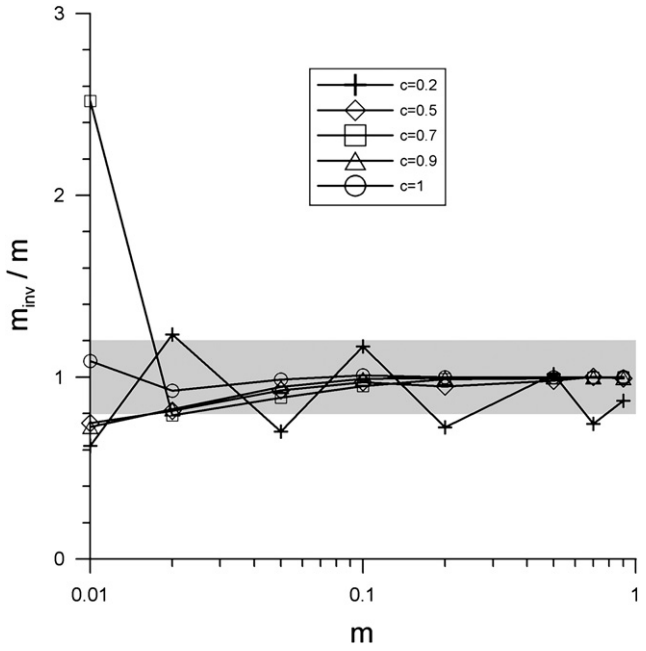

Fig. 3. Plots of the m_{inv}/m ratio versus "true" chargeability m. Symbols of curves are keyed according to the exponent c.

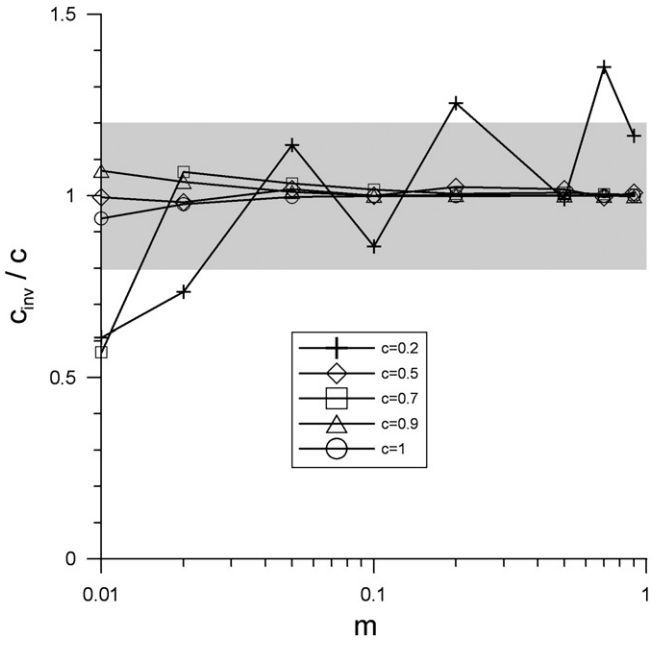

Fig. 5. Plots of c_{inv}/c ratios versus "true" chargeability m. Symbols of curves are keyed according to the exponent c.

approach provided an elegant illustration of how the inversion quality varies depending on specific independent parameter.

For better visualization the parameters plotted along the vertical axis were normalized. The variables m, τ, and c denoted "true" parameters, i.e., those used to compute the pseudo-empirical transients, and m_{inv}, τ_{inv}, and c_{inv} denoted the parameters found by inversion. The m_{inv}/m, τ_{inv}/τ, c_{inv}/c ratios measured relative difference between the inversion-derived and true parameters.

In Fig. 3 the m_{inv}/m ratios are plotted against the "true" chargeability m of the half-space. Symbols of the plots are specified according to the exponent c for the respective synthetic transients. Fig. 3 demonstrates how the inversion quality for m depends on the "true" chargeability and exponent. The closer the m_{inv}/m ratio to unity the better is the quality of recovering m by inversion. The gray bar corresponds to the area where the inversion error is no worse than ±20%. This error is in many cases acceptable in resistivity surveys and is an excellent result for inversion of Cole–Cole parameters.

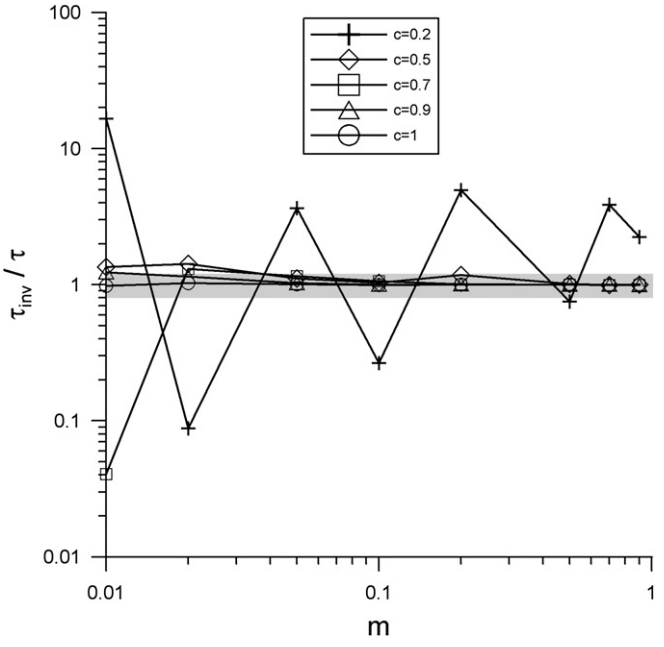

Fig. 4. Plots of τ_{inv}/τ ratio versus "true" chargeability m. Symbols of curves are keyed according to the exponent c.

The quality of m inversion improves with increasing chargeability m and exponent c, while the latter has a greater control. At $c=0.2$, the error is the largest and oscillates as a function of "true" chargeability. A large error at $c=0.7$ in the range of low m appears a somewhat unexpected result in view of the general tendency for a decrease in the inversion error with increasing c.

Fig. 4 shows the effect of m and c changes on the inversion quality for the IP relaxation time constant τ. Recall that for all models used in calculating pseudo-empirical data the true time constant τ had the same value of $5\cdot10^{-5}$ s. At $c=0.2$, the ratio τ_{inv}/τ oscillates quite strongly but the oscillation amplitude decreases with increasing chargeability. Because τ_{inv}/τ varied over two orders of magnitude at low m and $c=0.2$, we used logarithms of τ_{inv}/τ ratio in plotting $\tau_{inv}/\tau=f(m)$ graphs.

In the range of model parameters defined by $c>0.2$ and $m\geq0.05$, the difference between τ_{inv} and $\tau=5\cdot10^{-5}c$ did not exceed ±20%, which appears to be a good or very good inversion quality. As in the previous example, the quality of τ inversion was unexpectedly worse in the model with $c=0.7$ and $m=0.01$ than in that with $c=0.5$ and $m=0.01$.

Finally, we plotted c_{inv}/c as a function of m and c. The quality of c inversion was better than the inversion of m and especially τ (compare Fig. 5 with Figs. 3 and 4). Even at $c=0.2$, four of seven inversion-derived c values differed from the "true" ones for no more than ±20%. Again, the c_{inv}/c ratio oscillates and departs most from unity at $c=0.2$. For models with their parameters within the range constrained by $c>0.2$ and $m>0.02$, the error in c inversion didn't exceed a few percent.

5. Discussion

Although the convenient form to present its results remained problematic, it was apparent that inversion without prior information was of quite a low quality in some cases. At low m and c the non-

Table 3
The Cole–Cole parameters of the half-space models used to compare the efficiency of separate and joint inversion when applied to the pseudo-empirical coincident-loop (50 m×50 m) and central-loop (200 m×200 m transmitter and 50×50 m receiver loop) data

Model, N	1	2	3	4	5
ρ, Ω m	100	200	500	1000	2000
m	0.1	0.02	0.2	0.05	0.5
τ, s	$5\cdot10^{-5}$	10^{-4}	$2\cdot10^{-4}$	10^{-5}	$2\cdot10^{-5}$
c	0.6	0.7	0.4	0.9	1

polarizable layered earth models could fit the pseudo-empirical TEM responses with the least-squared fit error close to the EM noise-related measurement error. Increasing m and/or c required inversion in terms of polarizable layered earth models the parameters of which were often far from those of underlying true models.

At first glance it would seem that there is little if any correlation between true models and those recovered through the inversion. But the closer inspection of the inversion results suggests that this is not always the case. This is evidenced by those inversion results in Fig. 2a–e that have indicated IP. Although the recovered models were found to be two- or three-layer ones, two of five polarizable earth models were determined as an uniform half-space with $\rho=10^3$ Ω m, and in the three other cases the layer resistivities ρ were close, in the order of magnitude, to 10^3 Ω m. Although the two- and three-layer models had only the upper layer polarizable, it was thick enough (130 m–400 m) to be considered as a uniform polarizable half-space. The inversion error for the IP time constant τ was no worse than 20% in four of five models in Fig. 2a–e, and that for the exponent c was vanishing. Inversion for chargeability was the least accurate but remained within acceptable quality limits in view of the variability known in unconsolidated frozen rocks and other geological materials.

Inversion with some prior information gave the Cole–Cole parameters to an error no worse than ±20% at m above a few percent and $c>0.2$ (see the results presented in a form convenient for imaging and consideration in Figs. 3–5). Usually m and c values measured on unconsolidated frozen rocks (Frolov, 1998; Bittelli et al., 2004) satisfy the above inequalities. Thus, frozen ground appears to be an advantageous target for investigating the effects of fast-decaying induced polarization on the TEM response.

6. Numerical experiment: second stage

Recall that the objective of the second stage was to assess the efficiency of *joint inversion* of data measured with two loops of *different* sizes.

At this stage of the numerical experiment we used five models of uniform polarizable half-space. The Cole–Cole parameters were selected from ranges typical of frozen unconsolidated rocks (Frolov, 1998): $\rho=10^2$–$2\cdot10^3$ Ω m, $m=0.02$–0.5, $\tau=10^{-5}$ s–$2\cdot10^{-4}$ s, and $c=0.4$–1. The choice of parameters from the above ranges was made random in order to avoid any personal biases, especially toward a "favorable" combinations of parameters, i.e. such ones at which a good quality of inversion would be expected for certain. See the list of thus generated models in Table 3.

With each of the five models, the transients were computed for a central-loop (200 m×200 m transmitter and 50 m×50 m receiver) and for a 50 m×50 m coincident-loop configurations. The above size of the central-loop configuration was chosen because it corresponded to the usual practice of TEM soundings. The choice of the 50 m×50 m coincident loop was defined by two reasons. First, due to the transmitter loops differed in size by the factor of four, it was safe to assume that relative contributions to the total transient response from vortex and IP currents should differ substantially for the configurations chosen, and

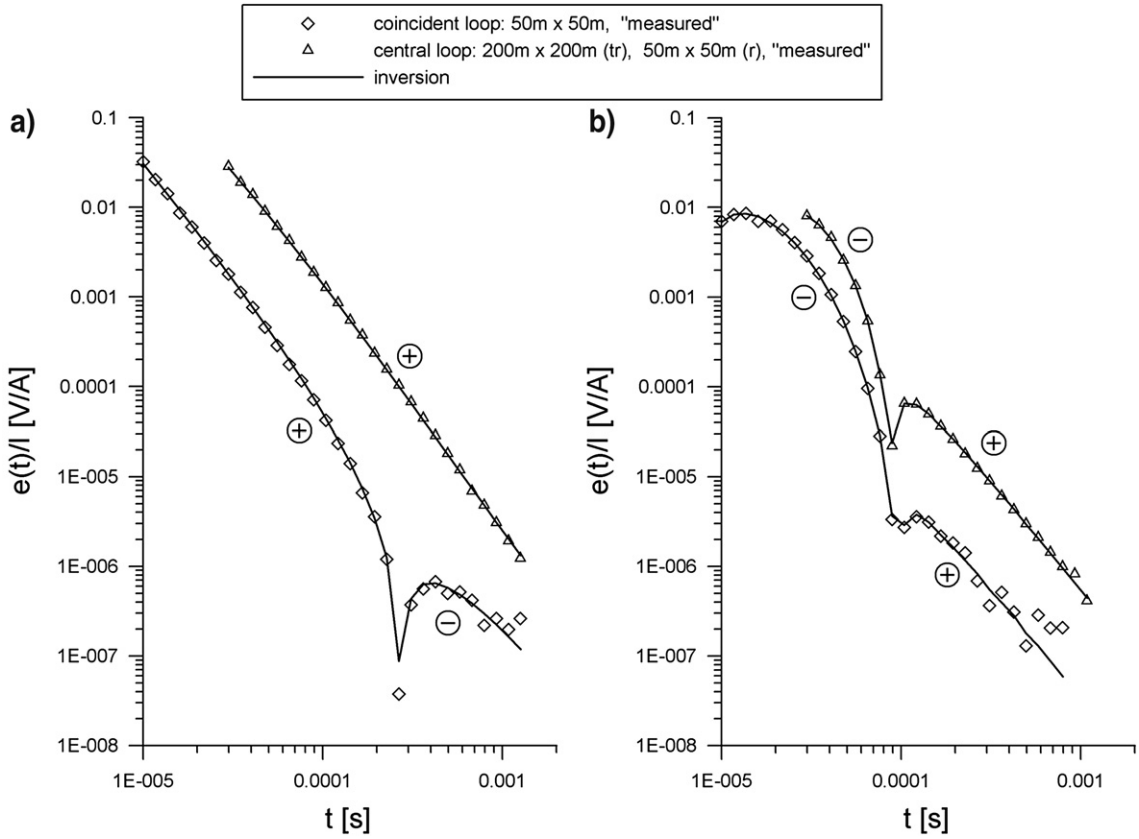

Fig. 6. Pseudo-experimental and fitted voltage transient responses: (a) model 3, (b) model 5 (Table 3). Plus and minus in a circle mark, correspondingly, positive and negative portions of transients.

this is a good prerequisite for joint data inversion (Kamenetsky et al., 1990). Second, the use of such configuration would not cause much problem in the field as it is easy to lay another 50 m×50 m loop once a central-loop configuration with 50 m×50 m receiver loop has been already set up.

As at the first stage of our simulation experiment, at the second one the synthetic transients were contaminated with Gaussian random noise. The field practice with the TEM method indicates that a larger transmitter loop usually provides a greater moment than a smaller one. Therefore, Author#1, who generated the pseudo-experimental data, assumed that the relative standard errors from the external EM noise were $\sigma_n=0.02$ for the central-loop configuration and $\sigma_n=0.05$ for the coincident-loop configuration. The internal noise, which is controlled by TEM measurement device and is independent of loop configuration, were taken the same as during single inversion (zero mean and $\sigma_n=0.1$ μV).

The time range of the generated pseudo-empirical transients was controlled by the transmitter loop size and instrumental facilities. According to our field experience, the transient self-response of the TEM system decay at 10 μs for the 50 m×50 m coincident-loop configuration and at 30 μs for central-loop configuration with 200 m×200 m transmitter and 50 m×50 m receiver loops. Although the latest delay time for all calculated transients was 100 ms, the latest times actually used in inversion varied depending on resistivity of half-space and did not exceed 1.3 ms for the coincident-loop configuration and 6 ms for the central-loop configuration. At these delay times the TEM voltage responses became less than 0.1 μV in order of magnitude.

Fig. 6 shows pseudo-empirical transients and those obtained through joint inversion for models 3 and 5 (Table 3). In the case of Fig. 6a, the smaller-loop transient unambiguously indicates the presence of fast-decaying IP (monotony break and sign reversal at 260 μs), while that measured with the large central-loop configuration looks in quite a normal way, i.e., emf remains positive and no IP effect appears. This response can be *formally* interpreted in terms of an equivalent non-polarizable 1D earth model.

Both transients in Fig. 6b show sign reversal: at 105 μs for the smaller coincident-loop configuration and at 90 μs for the larger central-loop configuration. Note that for this model in both cases the sign reversal is from a negative to a positive emf. The Cole–Cole relaxation time constant τ for model 5 being as short as 20 μs, the first sign reversal occurs too early to be measured with the 50 m×50 m coincident-loop configuration, and more so, with the central-loop configuration having a large transmitter loop.

The joint inversion differed from the single inversion in that Eq. (3) for the objective function included data for both configurations, i.e., $N=N_1+N_2$, where N_1 is the number of data for the large configuration and N_2 is that for the smaller one. Unlike the single inversion, during the joint inversion the forward operator F_p comprised the operators F_{p1} and F_{p2}. The former operator was used to compute the central-loop transient response whereas the latter one was used to compute the coincident-loop transient response. The measurement errors $\delta(t_i)$ included in Eq. (3) were different in the two loop configurations (see above), but Author#2 who did the inversion knew nothing of the features of the noise used to contaminate synthetic TEM responses. Therefore, he assumed 5% Gaussian noise to be present in all pseudo-empirical data, i.e. in those "measured" both with coincident-loop and central-loop configurations.

It is pertinent to write a few words about the relative contributions of transients from both configurations into the joint objective function. As we mentioned above, the transient responses generated with large transmitter loop could be "measured" at later times than those generated with the smaller transmitter loop. On the other hand, the configuration with smaller transmitter loop can resolve signals at earlier times than that with larger transmitter loop. The difference was not great though the number N_1 of data "measured" with the 200 m×200 m transmitter loop was usually greater than N_2, the number of data "measured" with the 50 m×50 m transmitter loop. Practically, the statistical weight of both data sets appeared to be nearly identical.

7. Results and discussion

As at the first stage of our simulation experiment, during the second stage the pseudo-empirical transients were inverted first without any knowledge of the underlying models. In view of Author#2 who did the inversion the synthetic transients had to be best inverted in terms of the two-layer polarizable earth model. At first coincident-loop and central-loop transients were inverted separately and then the data from both configurations were inverted jointly.

The inversion results are given in Table 4. First three models consisted of a polarizable basement overlain by a non-polarizable layer, both upper layer and basement were found to be polarizable in the fourth model, and the fifth model consisted of a polarizable layer above a non-polarizable basement. The relative mean-square deviation between quasi-empirical transients and those best fitting them was in a range of 2.5 to 42% and did not exceed 10% for eleven of fifteen models found through the inversion (Table 4).

Once inversion without prior information had been completed, Author#2 was told that all models were presented by a uniform polarizable half-space whereupon the inversions were run once again. See the respective columns of Table 5 for the recovered model parameters and relative standard errors.

Following the logic of the simulation experiment let us first discuss the inversion results obtained without prior information. Again one might find these results discouraging as the inversion resulted in a two-layer model with one or two polarizable layers instead of a uniform polarizable half-space.

However, a closer look at the upper layer thicknesses (Fig. 7 a) shows that the recovered models are not as bad as it may seem. For

Table 4
The results of separate and joint inversions done in the absence of prior information: coin loop–coincident loop; in loop–central loop

	Model 1			Model 2			Model 3			Model 4			Model 5		
	Coin loop	In loop	Joint	Coin loop	In loop	Joint	Coin loop	In loop	Joint	Coin loop	In loop	Joint	Coin loop	In loop	Joint
H_1, m	18	4.3	0.1	4.1	0.7	0.13	7.8	4.8	0.44	97	230	228	2.3	11.8	160
ρ_1, Ω m	82	62	42	174	290	185	240	202	217	1004	990	992	970	999	1390
m_1	0	0	0	0	0	0	0	0	0	0.047	0.049	0.053	0.7	0.67	0.45
τ_1, μs										10	13	10.4	38	38	17
C_1										0.92	0.94	0.91	0.99	0.95	0.98
ρ_2, Ω m	135	106	100	204	201	200	540	537	494	1040	1040	1040	2000	1960	3000
m_2	0.03	0.07	0.12	0.05	0.03	0.08	0.14	0.13	0.15	0.05	0.04	0.04	0	0	0
τ_2, μs	23	19	38	14	5.6	1.2	3.1	400	190	1	0.3	0.69			
c_2	0.44	0.41	0.55	0.42	0.39	0.35	0.54	0.54	0.53	0.84	0.89	0.91			
σ, %	6.1	4	7.1	5	3	6.4	24	2.4	18.4	4.7	3.2	5.7	30	9	42

For the underlying "true" models see Table 3.

Table 5
The results of separate and joint inversions done with regard to prior information: coin loop–coincident loop; in loop–central loop

	Model 1			Model 2			Model 3			Model 4			Model 5		
	Coin loop	In loop	Joint	Coin loop	In loop	Joint	Coin loop	In loop	Joint	Coin loop	In loop	Joint	Coin loop	In loop	Joint
ρ, Ω m	91	100	100	200	202	200	515	495	494	1040	1030	1000	1990	2000	2000
m	0.75	0.83	0.14	0.04	0.033	0.016	0.14	0.14	0.14	0.037	0.002	0.05	0.5	0.5	0.5
τ, μs	0.6	0.2	26	20	0.3	130	210	290	200	11	0.4	10.5	20	20	20
c	0.42	0.42	0.48	0.4	0.24	0.7	0.54	0.53	0.54	0.96	0.99	0.9	1	1	1
σ, %	6.4	4	7.1	5.5	3.3	5.7	26	2.5	22.6	5	4.3	6	25	5.4	21

For the underlying "true" models see Table 3.

models 1, 2, 3 with a non-polarizable layer overlaying a polarizable basement, the upper layer had a thickness H_1 much less than the transmitter loop size r. Therefore, the models 1, 2, and 3 can be approximated by a uniform polarizable half-space the parameters of which are the same as those of basements of above three models. Practically, inversion for models 1, 2, 3 gave a uniform polarizable half-space with $\rho=\rho_2$, $m=m_2$, $\tau=\tau_2$, $c=c_2$ (Fig. 8).

Model 4 was found to be represented by a two-layer earth with the polarizable layer (ρ_1, m_1, τ_1, c_1) overlying a polarizable basement (ρ_2, m_2, τ_2, c_2). The thickness of the upper layer H_1=100–230 m exceeded the characteristic sizes of both transmitter loops (200 m×200 m and, more so, 50 m×50 m). The IP relaxation time constant being $\tau_2<1$ μs, one may assume that $m_2=0$ within the time range of TEM sounding method. Therefore, the model practically approached a uniform polarizable half-space with $\rho=\rho_1$, $m=m_1$, $\tau=\tau_1$, $c=c_1$ (Fig. 8).

Finally, model 5 was found to be represented by a polarizable layer with ρ_1, m_1, τ_1, c_1 overlying a non-polarizable basement with resistivity $\rho_2=2\cdot10^3$–$3\cdot10^3$ Ω m. Separate inversion of pseudo-empirical transients for the two loop configurations gave a thin upper layer which was not a satisfactory result. However, joint inversion gave for the upper layer the thickness of 160 m thus justifying again a uniform half-space approximation with $\rho=\rho_1$, $m=m_1$, $\tau=\tau_1$, $c=c_1$ (Fig. 8).

Fig. 7b–f presents the normalized parameters of models recovered during inversion. In Fig. 7b, e, f the quantities m_{inv}, τ_{inv}, and c_{inv} stand for the chargeability, the time constant, and the exponent of those layers which were used to approximate two-layered models with a uniform polarizable half-space (Fig. 8).

Resistivities deserve a special comment. Although the inversion resulted in a two-layered earth model instead of a homogenous half-

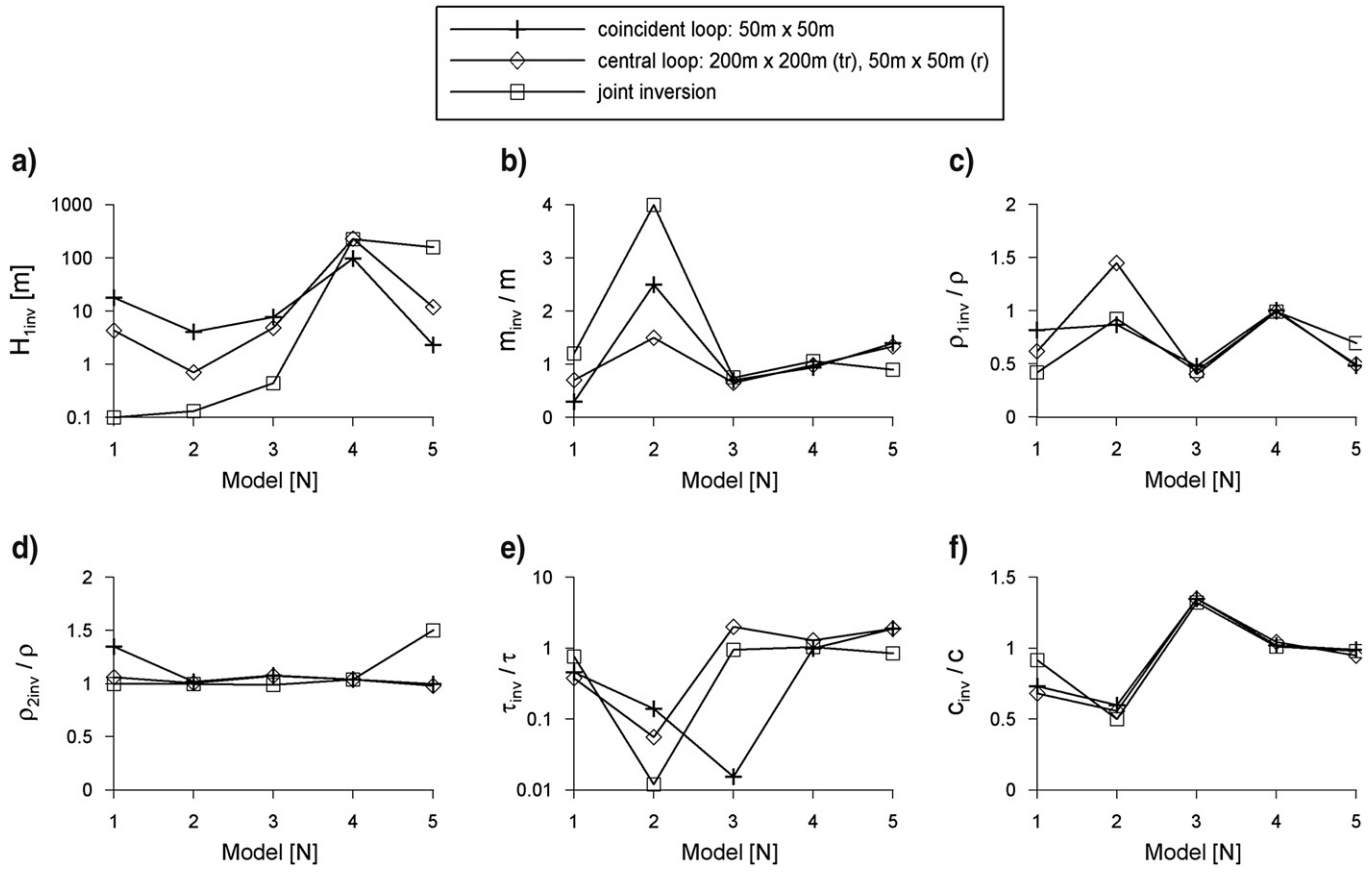

Fig. 7. Parameters of the two-layered models obtained by single and joint inversion plotted against the "true" model number (Table 3). Both single and joint inversions were done in the absence of prior information on the "true" models. Recovered parameters are: (a) H_{1inv}, thickness of the upper layer; (b) m_{inv}, chargeability of the polarizable layer; (c) ρ_{1inv}, resistivity of the upper layer; (d) ρ_{2inv}, resistivity of the underlying layer (basement); (e) τ_{inv}, relaxation time of the polarizable layer; (f) c_{inv}, exponent of the polarizable layer. The parameters of the relevant "true" half-spaces are denoted by ρ, m, τ, and c.

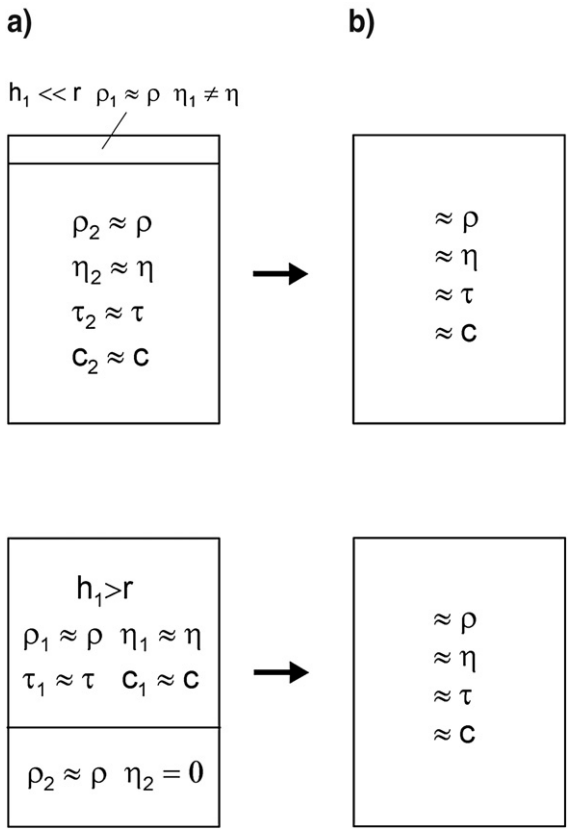

Fig. 8. Two-layer models obtained through inversion (a) and a homogeneous polarizable half-space they can be simplified to (b). With r is denoted the characteristic size of the TEM loop configuration: in the case being considered r is equal to a half of the transmitter loop size.

space, resistivities of both upper layer and basement were close to that of the "true" homogeneous half-space models. (Fig. 7c, d). Therefore, if our concern is just with resistivities, we should be content because all recovered models can be approximated by a homogenous half-space with resistivities close to those of the "true" models. From the point of view of a field geophysicist it means that practically the resistivity can be mapped to a reasonable accuracy even in the presence of strong fast-decaying IP and in the absence of prior information.

Looking at Fig. 7 it is not easy to decide unambiguously how much joint inversion is better than separate ones. The data in Fig. 7b, e, f indicate that the most problem was the inversion of pseudo-empirical transients for model 2 (Table 3). This is not particularly surprising since this model has very low (0.02) chargeability with its effect comparable to noise. That was the only model for which estimates of chargeability and time constant recovered from joint inversion appeared to be worse as compared to those found during separate inversions.

All in all, the advantage of joint inversion of the pseudo-empirical data for the models in Table 3 was as follows. The joint inversion reduced the thicknesses (by 10 to 100 times) of the upper non-polarizable layer for models 1, 2, 3 (Fig. 7a) and increased the thickness of the upper polarizable layer in model 5; something of the kind occurred for model 4 as well. Thus, joint inversion significantly biased the two-layer models towards the true homogeneous half-spaces.

The results of the inversion made with allowance for prior information are shown in Fig. 9 as normalized graphs. In should be noted first that with prior information given both separate and joint inversions resulted in correct resistivities. As for the other three parameters (m, τ, c), even with prior information given the separate inversion of both coincident and central-loop pseudo-empirical data resulted in rather large errors in the estimates of m, τ, c. However, after Author#2 was told that all five "correct" or "true" models were represented by a uniform polarizable half-space, joint inversion effectively shifted chargeability m (Fig. 9b), exponent c (Fig. 9d), and especially time constant τ (Fig. 9c) towards parameters of the true models. What's more, joint inversion with a minimum of prior information resulted in correct estimates of the parameters of the model 2, which was the hardest one in the case of separately inverting the synthetic TEM data.

Plots in Fig. 10 illustrate how the relative mean-square deviation σ between pseudo-experimental and predicted data changes depending on the "true" model (Table 3). As evident, σ varied from 2.5 to 30% in the absence of prior information and from 2.5 to 26% when prior information became available. In the former case, mean standard deviation was 14% for the coincident-loop data, 4.3% for the central-loop data, and 16% for joint inversion of both data. In the latter case mean standard deviation was found to be 13.6% for the coincident-loop configuration, 3.9% for central-loop configuration, and 12.5% for the joint inversion of both data.

The above estimates of σ and the plots shown in Fig. 10 allow the following inferences: (i) inversion of central-loop data results is σ values that are several times less than those obtained during inversion of both the coincident-loop data and joint inversion; (ii) for the most part models derived from joint inversion are closer to the "true" ones although σ remains about the same as in the case of separate inversion of the 50 m×50 m coincident-loop data; (iii) the availability of prior information, especially when doing joint inversion, allows a better recovery of the true models but the resulting σ values are close to those obtained during single inversions.

Thus, it may be safely suggested that, at least within the framework of the discussed simulation experiment, the 50 m×50 m coincident-loop data are critical in inversion of the TEM response to a uniform polarizable half-space. This inference is consistent with our earlier conclusion that inductively-induced polarization effect is relatively stronger in data measured with smaller loops (Kozhevnikov and Artemenko, 2004; Kozhevnikov and Antonov, 2006).

If chargeability is rather low and there is no prior information suggesting a polarizable earth, transients measured with large central-loop configuration can be accounted for in terms of a non-polarizable 1D earth, whereas data measured with a smaller coincident-loop configuration cannot be interpreted without invoking IP effects even at moderate chargeabilities.

At this point it is pertinent to discuss the cause of large fitting errors resulted from single inversion of 50 m×50 m coincident-loop data (on average, 14%) and from joint inversion (on average, 15%)? According to the experience we have gained during the reported simulation experiment, the primary cause is that some portion of the voltage response of 50 m×50 m coincident-loop configuration to polarizable half-space usually exhibits monotony break or even sign reversals (Fig. 6). Within this portion of the transient response, emf changes very rapidly with time and its values become vanishing in the vicinity of the sign reversal point. This portion of the TEM response being the main "carrier" of the IP-related information is, in addition, very sensitive to slight changes in the parameters of a model being recovered via inversion procedure. Thus, in the case of a polarizable earth, even minor changes in model parameters may cause large mean-squared deviation between predicted and pseudo-experimental TEM data. Because the discussed numerical experiment was designed to simulate real field TEM surveys, time delays used in our simulation were about the same as those used in most commercially-available TEM instruments. The time sampling interval of these instruments is sufficiently small to resolve relatively smooth voltage TEM response to non-polarizable conducive earth, but this is not always the case for polarizable earth. Fitting IP-affected TEM data, especially those with monotony break and/or sign reversals, requires a sampling interval sufficiently small for adequately resolving rapidly changing transient voltage.

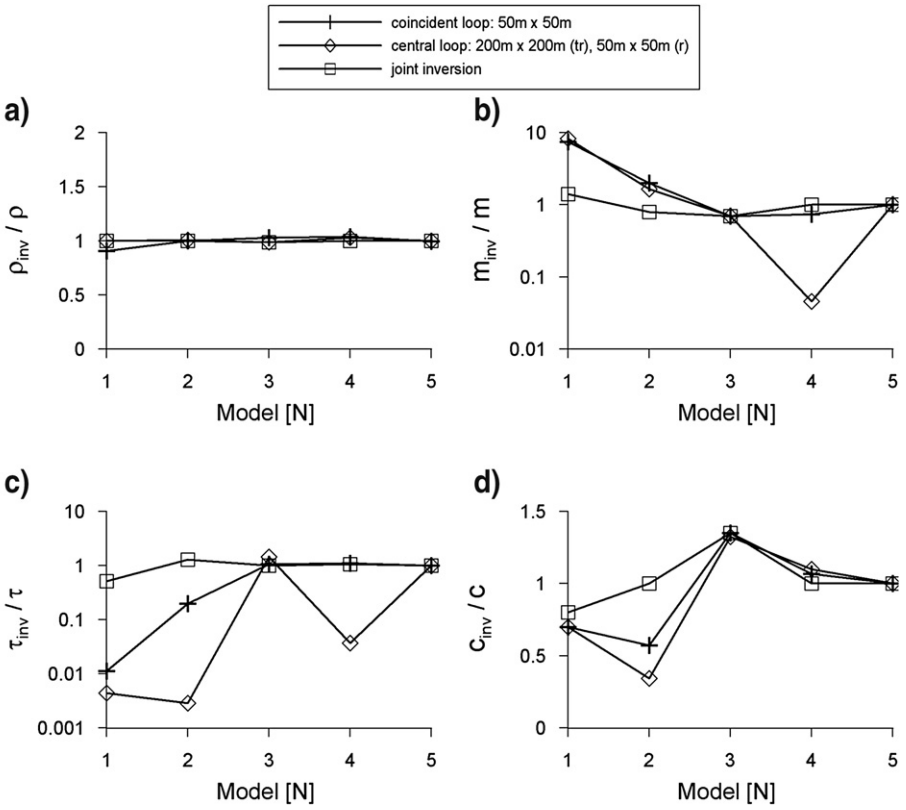

Fig. 9. Parameters obtained by separate and joint inversions of pseudo-experimental TEM responses as a function of the "true" model number (Table 3). The Author#2 who did the inversion was told that all "true" models were represented by a homogeneous polarizable conductive half-space. Recovered parameters are: (a) ρ_{inv}, the resistivity; (b) m_{inv}, the polarizability; (c) τ_{inv}, the relaxation time; (d) c_{inv}, the exponent. The parameters of the relevant "true" half-spaces are denoted by ρ, m, τ, and c.

Because transients measured with a large transmitter loop are less strongly affected by fast-decaying IP, the large loop data are especially important for improving the stability of inversion-derived resistivities, particularly as the relative measurement errors are smaller for the large transmitter loop (see above).

8. Field data inversion example

It should be recalled that the aim of our paper is first of all to get an idea on what one can expect when inverting the TEM signals measured over a homogeneous, polarizable half-space. A homogeneous half-space is a very simple model but in spite of or rather just because of this it is a fundamental one that provides a basis for understanding of how does a specific geophysical method work. Obviously one should not skip over a homogeneous half-space when learning to invert TEM transients measured over polarizable earth.

Although it was not among the main objectives of this paper to tackle with inversion of the field TEM data, we believe it would be of interest to give, as an example, some in-field-measured TEM data that could be modeled with a polarizable half-space.

Fig. 11 illustrates the inversion results for the TEM data measured at two sites in the vicinity of the city of Mirny in Western Yakutiya. The geology of the sites is represented by a thin layer of Quaternary unconsolidated sediments covering Jurassic sand and clay that are

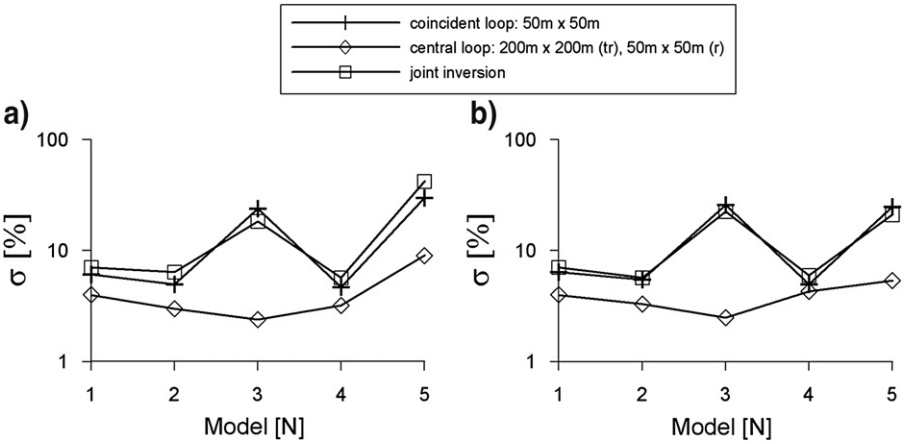

Fig. 10. Relative mean-square deviation between pseudo-experimental and predicted data plotted against the "true" model number (Table 3): (a) no prior information was known; (b) inversion with prior information.

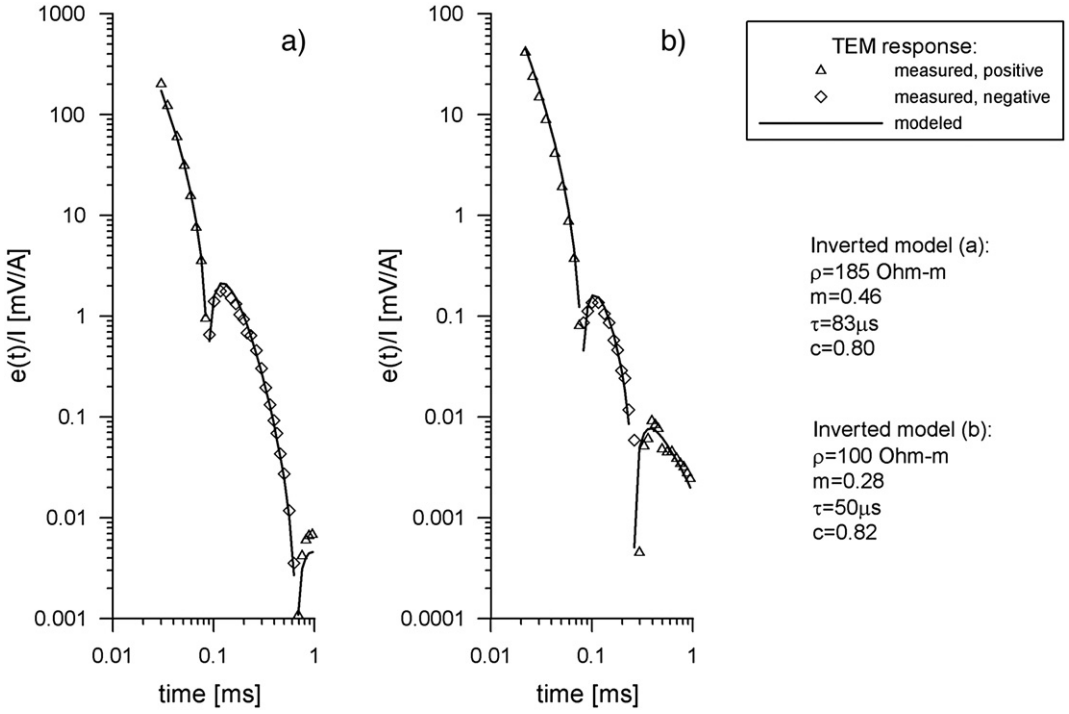

Fig. 11. Inversion of TEM responses measured in West Yakutiya, Russia: a) neighborhood of the city of Mirny, near a kimberlite pipe 'Imeni 23 s″ezda KPSS', 100 m × 100 m coincident-loop configuration; b) neighborhood of the city of Mirny, near a quarry, 50 m × 50 m coincident-loop configuration.

underlain by Lower Paleozoic terrigenous-carbonate sedimentary rocks.

The TEM signals were measured with 100 m × 100 m (Fig. 11a) and 50 m × 50 m (Fig. 11b) coincident-loop configurations. A commercially-available instrument Tzikl-5 (Elta-Geo, Novosibirsk) was used to produce and measure transients.

Open triangles and diamonds in Fig. 11 indicate the measured TEM signals and the solid line shows the 1D modeled responses. As one can see, TEM signals are influenced by the fast-decaying IP. The inverted models are shown on the right of Fig. 11. Geoelectrically, the earth here can be approximated by a homogeneous polarizable half-space the Cole–Cole parameters of which are typical of frozen ion-conductive rocks: ρ = 100–185 Ω m, m = 0.28–0.46, τ = 50–83 μs, c = 0.8. One of the reasons why the earth here is geoelectrically homogeneous has to do with the fact that being frozen ion-conductive rocks become more resistive and therewith less inhomogeneous in resistivity (Frolov, 1998).

It is argued in the paper of Smith and West (1989) that fast-decaying IP effects are more likely to be seen in areas where the ground is more conductive near to the surface so that the ground can be charged and the EM response will decay away more quickly. In other words, the conductive overburden better satisfies the "favorable coupling conditions" described by Smith and West. Although it is apparently true it does not mean that fast-decaying IP effects can not manifest themselves also in areas with other geoelectrical structures. Thousands of TEM signals indicating fast-decaying IP effects were measured in Yakutiya during diamond prospecting. However, being frozen, near-surface rocks in Yakutiya are not necessarily resistive and quite often fall far short of being 'conductive overburden'.

9. Conclusions

Understanding the utility of the inversion of TEM data affected by fast-decaying induced polarization is essential to the geophysicists working in northern areas and elsewhere in the world where one can expect fast-decaying IP to occur. We have tried to assess this utility by means of a numerical simulation experiment as applied to a uniform polarizable half-space with a conductivity described by the Cole–Cole model.

At low chargeability m and/or exponent c, pseudo-empirical transient response can be formally explained in terms of 1D non-polarizable conductive earth model; increasing m and/or c as well as decreasing the size of the loop configuration results in unambiguous IP manifestations.

More than a half of the recovered models, though some of them differ strongly from the underlying ones, provide a good idea of the "true" models; this is the case even for those models which were recovered from single inversion in the absence of prior information; the availability of even a small portion of prior information ensures a significantly better closeness to the "true" models.

As a rule, joint inversion of central-loop and coincident-loop data brings the model structure and Cole–Cole parameters closer to the true homogeneous half-space. With some prior information, joint inversion provides correct estimates of the Cole–Cole parameters even if the true chargeability is as low as only 0.02.

In the case that joint inversion is applied, squared error misfit between pseudo-experimental and predicted data vectors is controlled mainly by the fitting error for the smaller-loop data. This squared error distance is several times more than the EM-related measurement error, due to the fact that some portion of an IP-affected TEM response presents non-monotonous voltage changing very rapidly with time.

The reported results give additional support to the view that according to which effects of fast-decaying inductively-induced IP are "carriers" of useful geologic information (Molchanov et al., 1984; Smith and Klein, 1996; Svetov et al., 1996; Kozhevnikov and Antonov, 2006). Inversion of transients affected by fast-decaying IP in terms of the Cole–Cole model will contribute to the advantage of the TEM method, particularly in permafrost regions.

We believe the investigation of the utility of the inversion of TEM signals affected by fast-decaying IP has not to be restricted to the

homogeneous half-space. As indicated TEM survey in Western Yakutiya (Kozhevnikov and Antonov, 2006), a horizontally-layered polarizable earth is a promising candidate for further research.

Acknowledgments

The authors thank A. Hördt (the editor), R. Smith, and an anonymous reviewer for their helpful comments and suggestions which greatly improved both the general structure and the style of the paper. The study was supported by grant 07-05-00305 from the Russian Foundation for Basic Research.

References

Artemenko, I.V., Kozhevnikov, N.O., 1999. Modelling the Maxwell–Wagner effect in frozen unconsolidated rocks (in Russian). Kriosfera Zemli III (1), 60–68.

Bittelli, M., Flury, M., Roth, K., 2004. Use of dielectric spectroscopy to estimate ice content in frozen porous media. Water Resource Research 40 (1–11), W04212. doi:10.1029/2003WR002343.

Descloitres, M., Guerin, R., Albouy, Y., Tabbagh, A., Ritz, M., 2000. Improvement in TDEM sounding interpretation in presence of induced polarization. A case study in resistive rocks of the Fogo volcano, Cape Verde Islands. Journal of Applied Geophysics 45, 1–18.

El-Kaliouby, H.M., Hussan, A., El-Divany, E.A., Hussain, A., Hashish, E.A., Bayomy, A.R., 1997. Optimum negative response of a coincident-loop electromagnetic system above a polarizable half-space. Geophysics 62, 75–79.

Flis, F.M., Newman, G.A., Hohman, G.W., 1989. Induced-polarization effects in time-domain electromagnetic measurements. Geophysics 54, 514–523.

Frolov A.D. 1998. Electrical and elastic properties of ice and frozen ground (in Russian). Puschino, ONTI PSC RAN.

Kamenetsky, F.M., Sidorov, V.A., Timofeev, V.M., Yakhin, A.M., 1990. TEM processes in conductive polarizable earth. In: Kamenetsky, F.M., Svetov, B.S. (Eds.), Electromagnetic Induction in the Upper Crust (in Russian). Nauka, Moscow, pp. 14–40.

Karasev, A.P., Shesternev, D.M., Olenchenko, V.V., Yuditskikh, E.Yu., 2004. Simulation of fast electrochemical transient processes in frozen ground (in Russian). Kriosfera Zemli VIII (1), 40–46.

Kaufman, A.A., Keller, G.V., 1983. Frequency and Transient Soundings. Elsevier Science Publ. Co., Inc.

Komarov, V.A., 1980. Electrical Prospecting with the Induced Polarization Method (in Russian). Nedra, Leningrad.

Kormiltsev, V.V., Levchenko, A.V., Mesentsev, A.N., 1990. Estimating effect of induced polarization on the TEM response (in Russian). In: Kametsky, F.M., Svetov, B.S. (Eds.), Electromagnetic Induction Within the Upper Earth's Crust. Nauka, Moscow, pp. 86–87.

Kozhevnikov, N.O., Artemenko, I.V., 2004. Modelling the effect of dielectric relaxation in frozen ground on the results of transient electromagnetic measurements (in Rusian). Kriosfera Zemli VIII (2), 30–39.

Kozhevnikov, N.O., Antonov, E.Y., 2006. Fast-decaying IP in frozen unconsolidated rocks and potentialities for its use in permafrost-related TEM studies. Geophysical Prospecting 54, 383–397.

Kozhevnikov, N.O., Nikiforov, S.P., Snopkov, S.V., 1995. Field studies of fast-decaying induced polarization in frozen rocks (in Russian). Geoekologiya 2, 118–126.

Krylov, S.S., Bobrov, N.Yu., 2002. Application of the electromagnetic soundings for the investigation of frequency dispersion of the frozen ground's electrical properties (in Russian). Kriosfera Zemli VI (3), 59–68.

Lee, T., 1981. Transient response of a polarizable ground. Geophysics 46, 1037–1041.

Molchanov, A.A., Sidorov, V.A. (Eds.), 1985. Problems of Polarization of Rocks (in Russian), N 5847-85. VINITI Reports. 109 pp.

Molchanov, A.A., Sidorov, V.A., Nikolaev, Yu.V., Yakhin, A.M., 1984. New types of transient processes in TEM soundings. Izvestiya Earth Physics 20, 76–79.

Nelder, J.A., Mead, R., 1965. A simplex method for function minimization. Computer Journal 7, 308–313.

Shesternev, D.M., Karasev, A.P., Olenchenko, V.V., 2003. Early-time IP Surveys in Permafrost Areas (in Russian). Izd. SO RAN, Novosibirsk.

Sidorov, V.A., 1987. On the electrical polarizability of heterogeneous rocks. Izvestija of the Academy of Sciences of the USSR. Earth Physics N10, 58–64.

Sidorov, V.A., Yakhin, A.M., 1979. Induced polarization of rocks in TEM soundings. Izvestija of the Academy of Sciences of the USSR, Earth Physics N11, 46–52.

Smith, R.S., Klein, J., 1996. A special circumstance of airborne induced polarization measurements. Geophysics 61, 66–73.

Smith, R.S., West, G.F., 1989. Field examples of negative coincident-loop transient electromagnetic responses modeled with polarizable half-planes. Geophysics 54, 1491–1498.

Smith, R.S., Walker, P.W., Polzer, B.D., West, G.F., 1988. The time-domain electromagnetic response of polarizable bodies: an approximate convolution algorithm. Geophysical Prospecting 36, 772–785.

Spies, B.R., 1980. A field occurrence of sign reversals with the transient electromagnetic method. Geophysical prospecting 28, 620–632.

Spies, B.R., Frischknecht, F.C., 1991. In: Nabighian, M.N. (Ed.), Electromagnetic sounding. Electromagnetic methods in applied geophysics—Application, part A: Society of Exploration Geophysicists, vol. 2, pp. 285–426.

Svetov, B.S., Ageev, V.V., Lebedeva, N.A., 1996. Polarizability of rocks and high-resolution resistivity surveys (in Russian). Geofizika 4, 42–52.

Wait, J.R., 1982. Geo-Electromagnetism. Academic Press, Inc.

Vanchugov, V.A., Kozhevnikov, N.O., 1998. Investigating the geoelectrical structure of the Nakyn kimberlite field in Western Yakutiya with the TEM method (in Russian). In: Uchitel, M.S. (Ed.), Geology and Exploration of the Ore Deposits. Technical University of Irkutsk, pp. 164–176.

Walker, G.G., Kawasaki, K.K., 1988. Observation of double sign reversals in transient electromagnetic central induction soundings. Geoexploration 25, 245–254.

Weidelt, P., 1983. Response characteristics of coincident loop transient electromagnetic systems. Geophysics 48, 1325–1330.

Zadorozhnaya, V.Yu., Lepeshkin, V.P., 1998. TEM sounding of polarizable layered subsurface (in Russian). Izv. RAN, ser. Fizika Zemli, vol. 4, pp. 55–61.

Zhandalinov, V.M. 2005. EM transients in the search for kimberlite inWestern Yakutia, Russia (in Russian). Author's Abstract, PhD Thesis, Novosibirsk, 20 pp.